September 20-23, 2011
City of Cuernavaca México
XI International
Hydrogen Congress
an event of The Mexican Hydrogen Society
Cuernavaca...
The Endless Spring

PLATINUM DEPOSIT ON WO_x-C SYNTHESIZED BY DIFFERENT METHODS AS CATALYST IN PEMFC

M. L. Hernández-Pichardo[1,*], R. G. González-Huerta[2], S. P. Paredes-Carrera[1], J. A. Frías-Rojas[1], E. Palacios-González[3], P. del Angel[3]
[1]IPN-ESIQIE, Laboratorio de Investigación de Fisicoquímica y Materiales, UPALM, 07738 México, D.F.
[2]IPN-ESIQIE, Laboratorio de Electrocatálisis, UPALM, 07738 D.F. México, D.F.
[3]Instituto Mexicano del Petróleo, DIyP, Eje Central L. Cárdenas 152, México, D.F.
[*] contact email: mhernandezp@ipn.mx

ABSTRACT

Practical catalysts for low-temperature fuel cells are typically in the nano-size range and are typically deposited on high-surface-area supports. Pt/C is the most commonly used catalyst for both cathode and anode in proton exchange membrane fuel cells (PEMFCs), however, some other catalysts such as Pt/MoO_x and Pt/WO_x are also considered promising, and therefore, this work is focused on the synthesis and characterization of nanostructured Pt/WO_x-C as both cathode and anode electrocatalysts for PEMFCs. The Pt deposit on the surface of the support is a crucial step in the synthesis of the catalytic materials, so then different synthesis methods were probed in order to find the conditions for the higher dispersion and accessibility of Platinum over the WO_x-C support and to improve the PEMFC cathode stability. The catalysts were prepared by UV and ultrasound assisted approaches, and characterized by Transmission Electron Microscopy and lineal and cyclic voltammetry.

Key words: Electrocatalysts, Platinum, WO_x nanostructures.

1. INTRODUCTION

Degradation of the catalyst support material in the cathode of the proton exchange membrane fuel cell (PEMFC) has been discussed recently. Previously some authors have reported on the corrosion of the catalyst-supporting carbon in the context of PEMFC. The cathodic PEMFC environment, including high acidity, electrochemical potential, water content as well as O_2 concentration, sets high demands on the catalyst support material. The presence of Pt on carbon increases significantly the rate of carbon corrosion. The carbon corrosion results in a decreased contact between the support and the Pt catalyst particles, which consequently become more mobile and might form larger Pt aggregates or migrate out of the cathode. Carbon degradation can also cause increased hydrophilicity of the supporting carbon, which results in deteriorated mass-transport properties of the cathode [1,2]. One current approach for eliminating carbon corrosion is to optimize operation conditions, e.g. avoidance of high humidity levels and high-voltage operation. Another approach is the development of more stable supporting carbons, such as graphitized carbon or the incorporation of some promoters to the catalytic system. WO_x promoted electrocatalysts are interesting to evaluate, not only due to its high stability at PEMFC cathode potentials in hydrous, acidic environment, but also due to recent reports on introducing W-containing materials into different electrodes [3-6].

WO_x structures have been reported to perform well as catalyst support in PEMFC cathodes and studies on electrodes, where the Pt has been deposited on C/WO_x, showed an increased electrochemically active area of Pt deposited on carbon in the presence of WO_x [7]. Savadogo et. al. [4,5] found that the catalytic activity of 40% WO_3-based electrode was higher than the 10% Pt-based electrode for the ORR. However they found that a mixture of anhydrous WO_3 also increases the electrochemically active surface area of the Pt dispersion on carbon, but the synergistic effect is significantly less than that observed with hydrated WO_3, i.e., tungstic acid. Some other authors has reported that the improvement of fuel cell performance and the increase of the electrochemically active surface area produced by the WO_s incorporation, are caused by synergistic effects between the platinum and oxides materials [6]. Therefore, as the role of the tungsten species is still somewhat debated, in this paper the incorporation of WO_x nanostructures

to Pt/C electrocatalysts through different methods was studied in order to determine the influence of the incorporation of WO_x nanostructures over the catalytic activity of Pt/C materials and in the PEMFC cathode stability.

2. EXPERIMENTAL

2.1 Electrocatalysts synthesis

Two Pt-WO_x/C electrocatalysts, and a blank Pt/C sample were prepared using platinum (II) acetylacetonate, $Pt(C_5H_7O_2)_2$, ammonium metatungstate, $(NH_4)_6W_{12}O_{39}{\cdot}xH_2O$), and Vulcan XC-72 carbon, with nominal contents: 10 wt. % Pt and 5 wt.% WO_3.

The Pt/C catalyst (*PtC*) was prepared by the photochemical deposition of Pt using a UV-vis lamp of 80 W during 3 h. The procedure of photodeposition method is briefly described as follows. The carbon was dispersed into an ethanol solution of platinum acetylacetonate ($5x10^{-4}$ M), the suspension was ultrasonically irradiated with 25 KHz of power during 15 min at room temperature and stirred vigorously by a magnetic stirrer during 1 h. The suspension was poured into the photo-reactor and the sample was irradiated for 3 h. Finally the product was washed with distilled water several times and dried at 70 °C by about 2 h.

The Pt-WO_x/C samples were prepared by two methods. The catalyst prepared by method I (*PtCW-I*) was prepared by the impregnation of the *PtC* sample with an ethanol solution of ammonium metatungstate ($1x10^{-5}$ M), the solution was stirred by 1 h at room temperature, then NH_4OH was added to reach pH 10. The product was washed repeatedly and then dried at 110 °C for about 2 h. This sample was labeled as *PtCW-I*.

The catalyst prepared by method II was synthesized by coprecipitation of Pt and tungsten and chemical reduction with sodium borohydride ($NaBH_4$). A solution of platinum acetylacetonate, ammonium metatungstate and ethanol was stirred with the respective portion of Vulcan XC-72 carbon during 1 h at room temperature; afterwards NH_4OH was added to reach pH 10. The product was washed repeatedly and then excessive $NaBH_4$ solution was added drop by drop and stirred for 3 h. Finally, the slurry was washed with distillated water, filtered and dried at 110 °C for about 2 h. This catalyst was denoted as *PtCW-II*.

2.2 Electrochemical Characterization

All electrochemical measurements were carried out at 25 °C in a single, conventional, three-electrode test electrochemical cell in a 0.5 M H_2SO_4 aqueous solution. A platinum mesh was used as the counter electrode, and Hg/Hg_2SO_4/0.5 M H_2SO_4 (MSE=0.680 V/NHE) as the reference electrode. Experiments were performed in a Potentiostat AutoLab PGSTAT12/30/302 and a Pine MSRX rotation speed controller. The potentials in this paper were related to normal hydrogen electrode (NHE). Rotating disk electrode (RDE) technique was employed for the purpose of determining the kinetic parameters. For RDE experiments, 8 µl of a sonicated mixture of 1mg of catalyst, 60 µl of ethyl alcohol (spectrum grade), 6 µl of distilled water and 6 µl of 5wt% solution Nafion® (Du Pont, 1000EW) were deposited on glassy carbon electrode (GC) with a cross-sectional area of 0.19 cm^2. The estimated amount of catalyst on the GC surface was about 0.58 mg cm^{-2}.

Before the ORR measurements, cyclic voltammetry (CV) was performed from 0.0 to 1.25 V at 50 mV s^{-1} in a nitrogen-saturated electrolyte, to clean the electrode surface. Forty cycles were necessary to stabilize the current–potential signal. Thereafter, the acid electrolyte was saturated with pure oxygen and maintained on the electrolyte surface during the RDE tests. Hydrodynamic experiments were recorded in the rotation rate range of 100 to 1600 rpm at 5 mV s^{-1}. Between RDE measurements, the acid electrolyte was saturated with pure oxygen for 10 minutes to obtain the stable open circuit potential. The current density was calculated using the geometric surface area.

2.3 Physicochemical characterization

To analyze morphology and particles distribution the samples were studied by high-resolution transmission electron microscopy (HRTEM), the micrographs were obtained in a TITAN 80-300 with Schottky type field emission gun operating at 300 kV. The point resolution and the information limit were better than 0.085 nm. HRTEM digital images were obtained using a CCD camera and Digital Micrograph Software from GATAN. In order to prepare the materials for observation, the powder samples were ultrasonically dispersed in ethanol and supported on holey

carbon coated copper grids. Pt and tungsten dispersion and local contents were studied by SEM using a Nova200 Nanolab, Dual Beam Microscope, Field Emission Scanning Electron Beam, which has 1.1 nm of resolution, and a Focused Ion Beam, with 1.7 nm of resolution.

3. RESULTS

3.1. Electrochemical Characterization

The cyclic voltammetry (CV) characterization of the platinum electrode in the supporting electrolyte was performed in a nitrogen purged 0.5 M H_2SO_4 solution, at a 50 mV s^{-1} scan rate. In this experiment, the electrodes were submitted to 40 cycles in order to obtain reproducible voltammograms. **Figure 1** presents voltammograms of the three platinum samples for comparison purposes. The PtC and PtCW-I electrodes present voltammograms with defined peaks associated with adsorption/desorption hydrogen, which are characteristics in polycrystalline noble metals. The voltammograms of the PtC and PtCW-I electrodes show similar surface reactions in a potential region of 0.0 V–0.3 V/NHE. Analysis at a more positive potential, corresponding to the anodic region, also shows a well-defined hydroxide-adsorbed peak with a slight difference in the current magnitude, which indicates that the both catalysts have a similar capacity for anion adsorption. Cathodic scan shows the same reduction potential of the oxides formed during anodic sweep. The reduction peaks of PtCW show a slight displacement to cathodic potential. The addition of carbon as electron conducting component compensates for the low electronic conductivity of WO_x.

On the other hand, the PtCW-II catalyst, **Figure 1**, shows a striking difference in the current magnitude in all potential scan. The PtCW-II presents an expected low electrochemically active area in the hydrogen region as well as low oxygen reduction activity and a decrease double layer capacitance; it is presumably due to a reduced direct contact between Pt and the reactants, produced by a coating of platinum with tungsten. Then, it is found that is better to synthesize WO_x to the Pt-C than synthesize to the Pt-WO_x-C together cathode performance of the composite electrode could be achieved in combination with an improved stability.

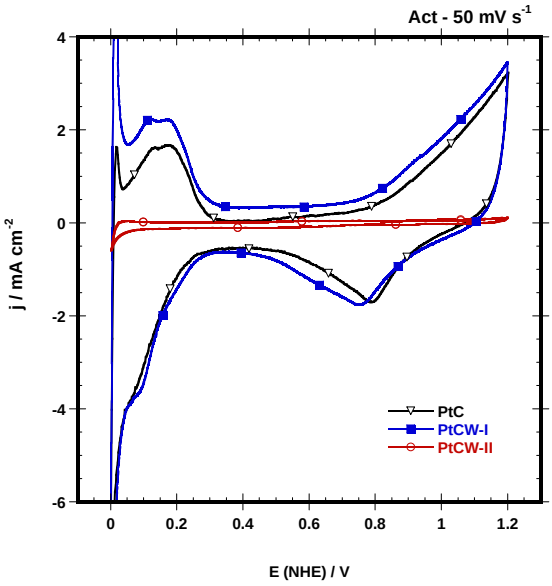

Figure 1. Cyclic voltammetry of PtC, PtCW-I and PtCW-II catalysts in O_2 free 0.5 M H_2SO_4 solution. Scan rate potential of 50 mVs^{-1}.

The polarization curves on PtCW-I, incorporated into a Nafion® film electrode, were performed at different rotation rates, in an oxygen-saturated 0.5 M H_2SO_4 solution at 25 °C, **Figure 2**. The polarization curves show three well defined potential zones: charge transfer, mixed and mass transport. It was considered that defined limiting currents are associated with the high diffusion of oxygen through the electrode surface and the uniform distribution of active sites. On the PtCW-I electrocatalyst, the oxygen reduction is fast enough that, at high over-potentials, a flat limiting plateau is observed. This phenomenon can be associated to a good distribution of the electrocatalytic sites on the electrode surfaces. On a film-coated electrode surface, the overall measured density current (j), is related to the kinetic density current (j_k), the boundary layer-layer diffusion-limited density current (j_d), and the film diffusion-limited current (j_f), by equation (1). The effect of the film diffusion is significant only in cases where the electrode is covered by the Nafion film and can be neglected in the present study since the amount of Nafion (0.94 µl 5 wt.% Nafion in 8 µl of solution) in the prepared catalyst suspension is sufficiently small. Hence, it should not be considered a factor in the limiting current density. Thus, the overall measured

current of the oxygen reduction can be written as being dependent on the kinetic current and the diffusion-limited current, as shown on the left side of the following equation:

$$\frac{1}{j} = \frac{1}{j_k} + \frac{1}{j_d} + \frac{i}{j_f} = \frac{1}{j_k} + \frac{1}{B\omega^{1/2}}$$

The kinetic current density is proportional to the intrinsic activity of the catalyst. The constant B is $0.2nFCD^{2/3}\nu^{-1/6}$, where 0.2 is a constant used when ω is expressed in revolutions per minute, C is the bulk concentration of oxygen (1.1×10^{-6} mol cm^{-3}), D is the diffusion coefficient of oxygen in the sulfuric acid solution (1.4×10^{-5} cm^2 s^{-1}), and v is the kinematic viscosity of the sulfuric acid (1.0×10^{-2} cm^{-2} s^{-1}).

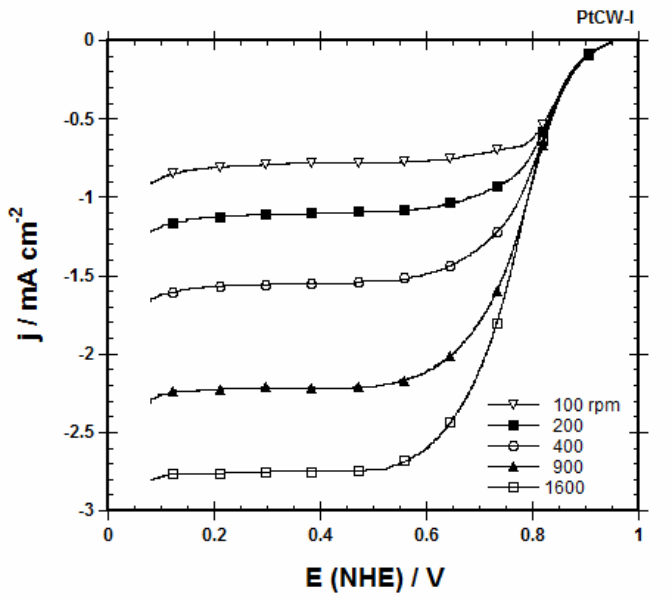

Figure 2. Polarization curves for PtCW-I in O_2 saturated 0.5 M H_2SO_4 at different rotation rates.

Figure 3 displays the ORR activity of PtC and PtCW-I at a rotating speed of 1600 rpm and 25 °C. The PtCW-II electrode showed very low oxygen reduction activity and the response in not included, in this figure. As observed in this figure, the ORR, in the activation region is more favorable for the PtCW-I catalyst and the current density is bigger than PtC. The inset in Figure 3 shows the mass-transfer-corrected Tafel plots for the PtC and PtCW-I. Tafel slope at low current density has a value of 76 mV dec^{-1} and 77 mV dec^{-1} respectively, which indicates that the first

electron transfer on the adsorbed oxygen molecule is the rate-determining step. This behavior is in agreement with results reported by other authors for PtC and PtCW-I catalysts prepared by other synthetic methods [8-10]. Table 1 summarizes all the kinetic parameters deduced for the ORR on the PtC and PtCW-I electrocatalysts.

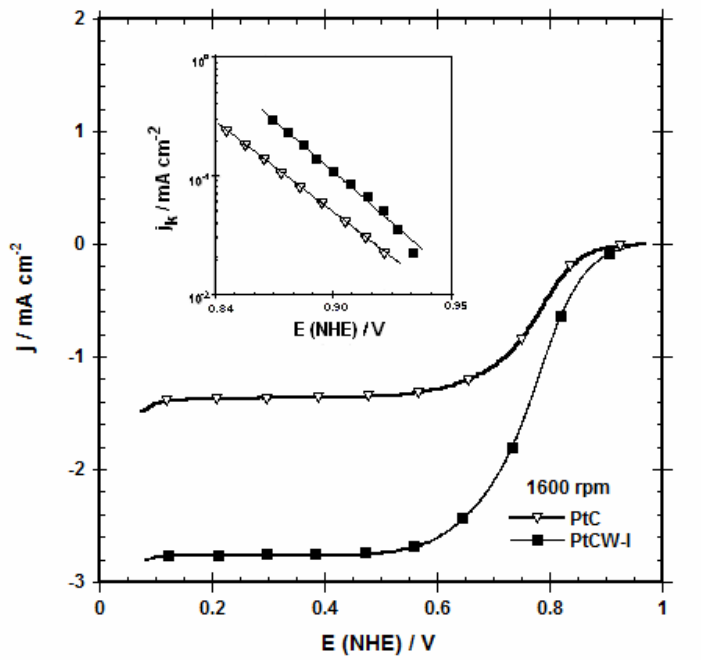

Figure 3. Comparison of the polarization curves in O_2 saturated 0.5 M H_2SO_4 at 1600 rpm and mass transfer corrected Tafel plots for the ORR on PtC and PtCW-I catalysts.

From Table 1 it is observed the same open circuit potentials to both analyzed samples, 0.97 V. The potentials at a current density of 0.1 mA cm^{-2}, were 0.88 V and 0.90 V to PtC and PtCW-I respectively. Therefore, the electrochemical results indicate that the incorporation of WO_x enhance the catalytic activity towards the ORR.

Table 1. Kinetic parameters deduced from Tafel slope in ORR on PtC and PtCW-I Catalysts.

Muestra	E_{ca} **V/ENH**	$-b$ **mV dec^{-1}**	α	j_o **mA cm^{-2}**	**Potential / V** j **=0.1 mA cm^{-2}**
PtC	0.97	77	0.76	2.86 x 10^{-6}	0.88
PtCW-I	0.97	76	0.77	5.78 x 10^{-6}	0.90

Figure 4, shows the results from the SEM analysis of the PtCW-I sample. The EDS coming from the region shown indicates a homogeneous dispersion of Pt, W, O and C, and this result was confirmed by the chemical mapping of the same area, as well as some other studied zones. It is observed that in this catalyst the Pt and tungsten signals are distributed over the entire surface, which indicates that these components are homogeneously dispersed on the surface. Interestingly, the Pt and tungsten content were lower that the nominal composition considered for the synthesis, due to the formation of platinum or tungsten oxides, from the uniform presence of oxygen over the entire sample.

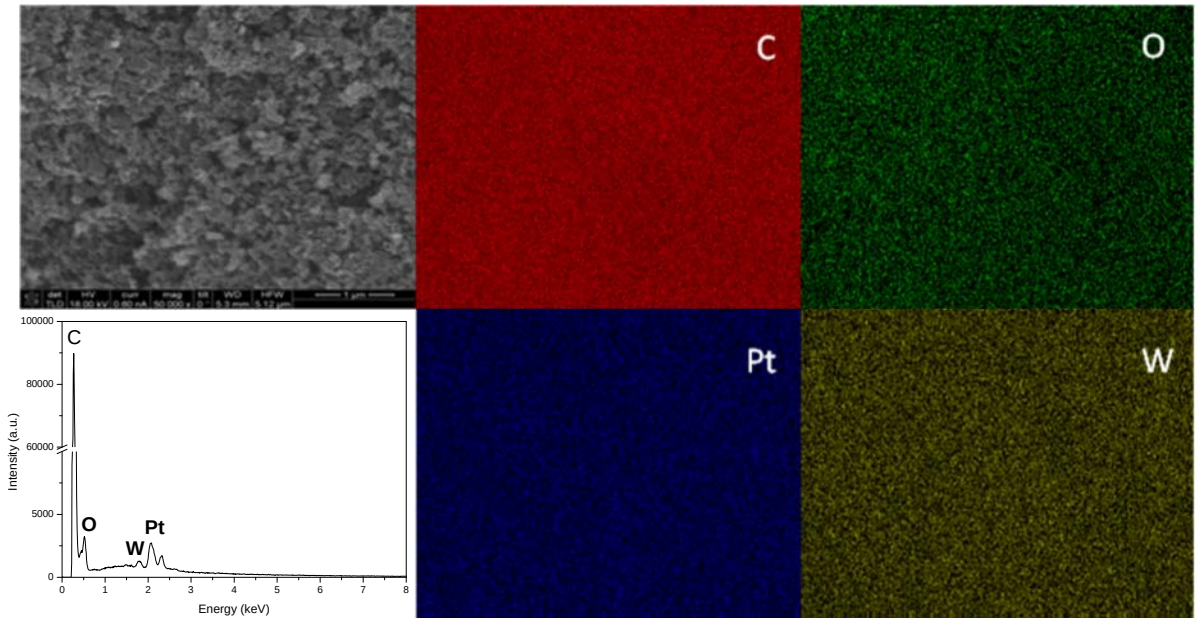

Figure 4. EDS and P, W, O and C chemical mapping of the PtCW-I catalyst.

TEM analysis was carried out on the PtCW-I catalyst to characterize the morphology and size of particles, **Figure 5**. It is noted that the material has a regular morphology. Pt particles have a uniform size and it is observed that they are uniformly impregnated with mean diameters at about 2-5 nm, in concordance with the SEM results. The physicochemical results indicate a good dispersion of the Pt and WO_x nanoparticles on the carbon surface produced by the synthesis method I, however it was difficult to identify the structure and coordination of the WO_x species. The tungsten oxide species present in an aqueous solution varies as functions of the pH of the

impregnating solution and concentration [11], the equilibrium between monomeric WO_4^{2-} and polymeric $W_{12}O_{42}^{12-}$ species. The tetrahedrally coordinated WO_4^{2-} is the predominant species in basic solution, in this case by adding NH_4OH in a controlled way, we observed the precipitation of a white gelatinous solid, then it is possible that these monomeric species with tetrahedral coordination interact with the reduced platinum during the precipitation producing a synergetic effect between these species (Method I), however, the coprecipitation of tungsten and platinum precursors decreases the catalytic activity of the Pt/C material, probably due to the tungsten species cover the Pt surface, avoiding the oxygen accessibility to the metallic particle.

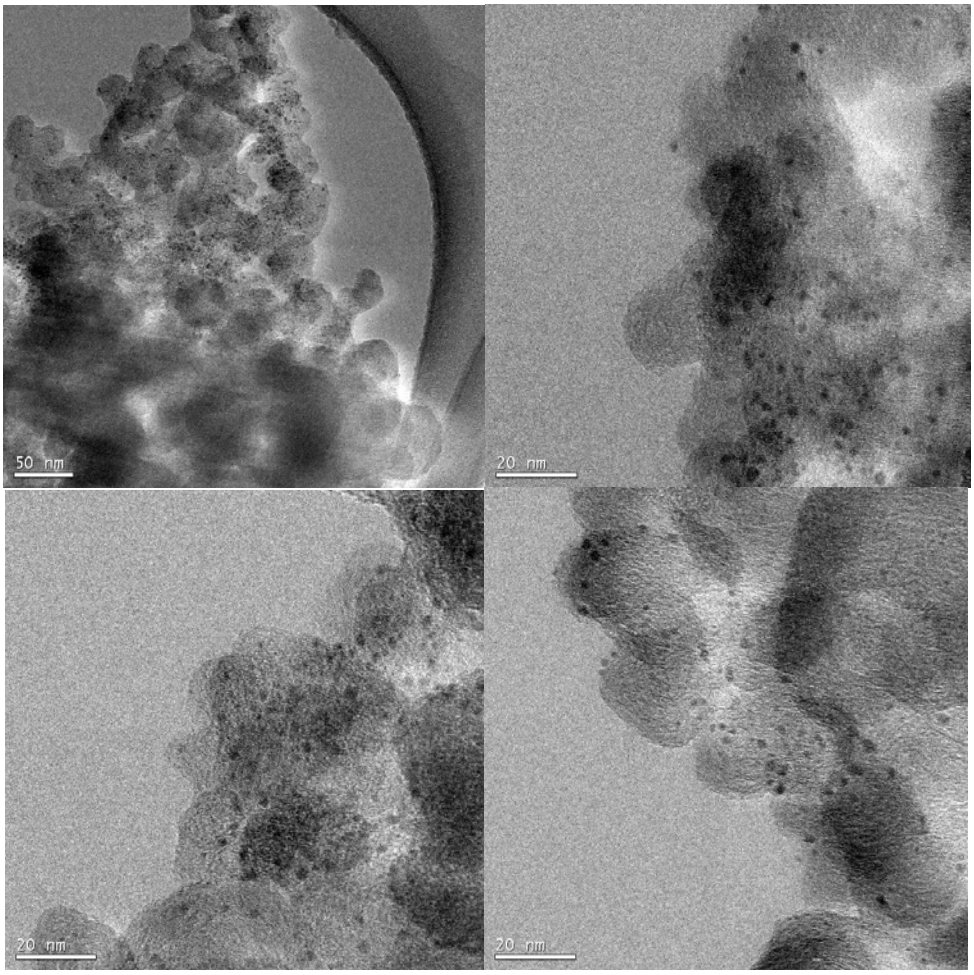

Figure 5. TEM images of the PtCW-I catalyst in different zones.

4. CONCLUSIONS

The results indicate that the higher activity of the PtCW-I sample prepared by the deposition of WO_x species on Pt/C generates a higher number of active size on the surface than the simultaneous precipitation of platinum and tungsten, probably due to a higher Pt dispersion along with the synergetic effect of Pt and the WO_x species. However, further studies about the tungsten composition and crystalline structure are needed.

Acknowledgements

Authors would like to acknowledge to the IPN for the grants and financial support received (SIP-20113593 and 20113657), as well as the CONACYT (Project 130254). The authors also acknowledge the facilities of the Electron Microscopy Laboratory of the Instituto Mexicano del Petroleo for this work.

5. REFERENCES TITLE

[1] L. Timperman, Y.J. Feng,W. Vogel and N. Alonso-Vante, *Electrochim. Acta*, **55**, 7558-7563 (2010).

[2] M.S. Saha, M.N. Banis, Y. Zhang, R. Li, X. Sun, M. Cai and F.T. Wagner, *J. Power Sources*, **192**, 330-335 (2009).

[3] A. K. Shukla, M. K. Ravikumar, A. S. Arico, G. Candiano, V. Antonucci, N. Giordano and A. Hamnett, *J Appl Electrochem*, **25**, 528-532 (1995).

[4] O. Savadogo and P. Beck, *J. Electrochem. Soc*., **143**, 3842-3846 (1996).

[5] O. Savadogo and A. Essalik, *J. Electrochem. Soc*., **143**, 1814-1821 (1996).

[6] J. Shim, Ch. Lee, H. Lee, J. Lee and E. J. Cairns, *J. Power Sources*, **102**, 172-177 (2001).

[7] Z. Cui, L. Feng, Ch. Liu and W. Xing, *J. Power Sources*, **196**, 2621-2626 (2011).

[8] Y. Wang, S. Song, V. Maragou, P. K. Shen and P. Tsiakaras, *Appl. Catal. B: Environmental*, **89**, 223-228 (2009).

[9] M.S. Saha, M.N. Banis, Y. Zhang, R. Li, X. Sun, M. Cai and F.T. Wagner, *J. Power Sources*,**192**, 330-335 (2009).

[10] E. Antolinia and E. R. Gonzalez, *Appl. Catal. B: Environmental*, **96**, 245–266 (2010).

[11] D. S. Kim, M. Ostromecki and I. E. Wachs, *Catal. Lett.*, **33**, 209-215 (1995).